Electronic Supplementary Material (ESI) for Soft Matter.

Supporting Information for: The rheology and foamability of crystal-melt suspensions composed of triacylglycerols

Kim Mishra,*,† Fabian Kämpf,† Silas Ehrengruber,† Julia Merkel,† Nico Kummer,‡,† Robin Pauer,‡ Peter Fischer,† and Erich J. Windhab†

†*Institute of Food, Nutrition and Health, ETH Zürich, Schmelzbergstrasse 9, 8092 Zürich*

‡*Laboratory for Cellulose & Wood Materials, EMPA – Swiss Federal Laboratories for Materials Science and Technology, Überlandstrasse 129, 8600 Dübendorf, Switzerland*

E-mail: kim.mishra@hest.ethz.ch

Phone: + 41 44 632 97 10

Contents

- Piping and instrumentation diagram of the crystallization and foaming process.
- Schematic drawing of the UVP-PD measurement set up.
- XRD spectra of AFM and CB and DSC thermograms of CB directly after crystallization
- SEM images of AMF, CB, and PKO crystallized at $\dot{\gamma}_{cryst} = 430\ \mathrm{s}^{-1}$
- SEM images of AMF, CB, and PKO crystallized at $\dot{\gamma}_{cryst} = 1075\ \mathrm{s}^{-1}$
- SEM images of AMF, CB, and PKO crystallized at $\dot{\gamma}_{cryst} = 2150\ \mathrm{s}^{-1}$
- Process settings during DEMF of TAG CMS
- The viscosity η as function of shear rate $\dot{\gamma}$ for TAG CMS

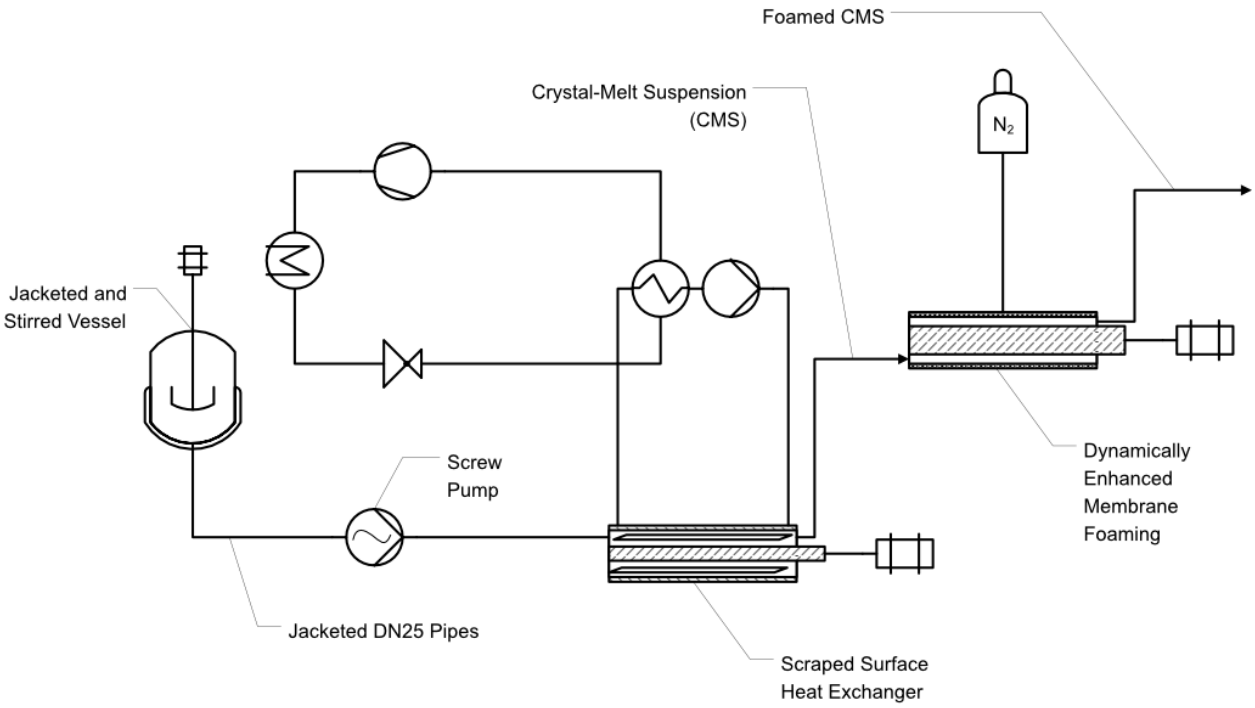

Figure S1: Piping and instrumentation diagram of the melt crystallization process and the subsequent dynamically enhanced foaming process.

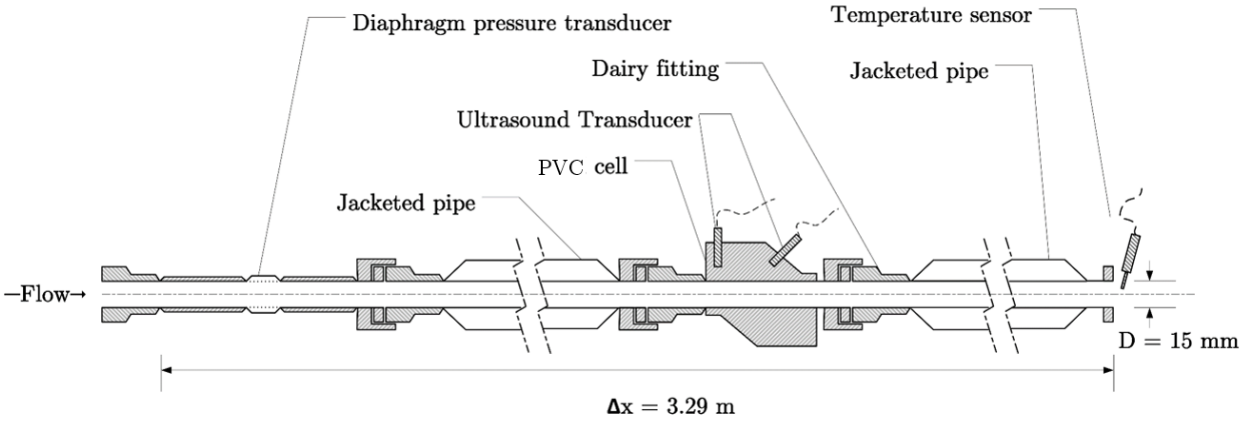

Figure S2: Schematic drawing of the UVP-PD measurement set up.

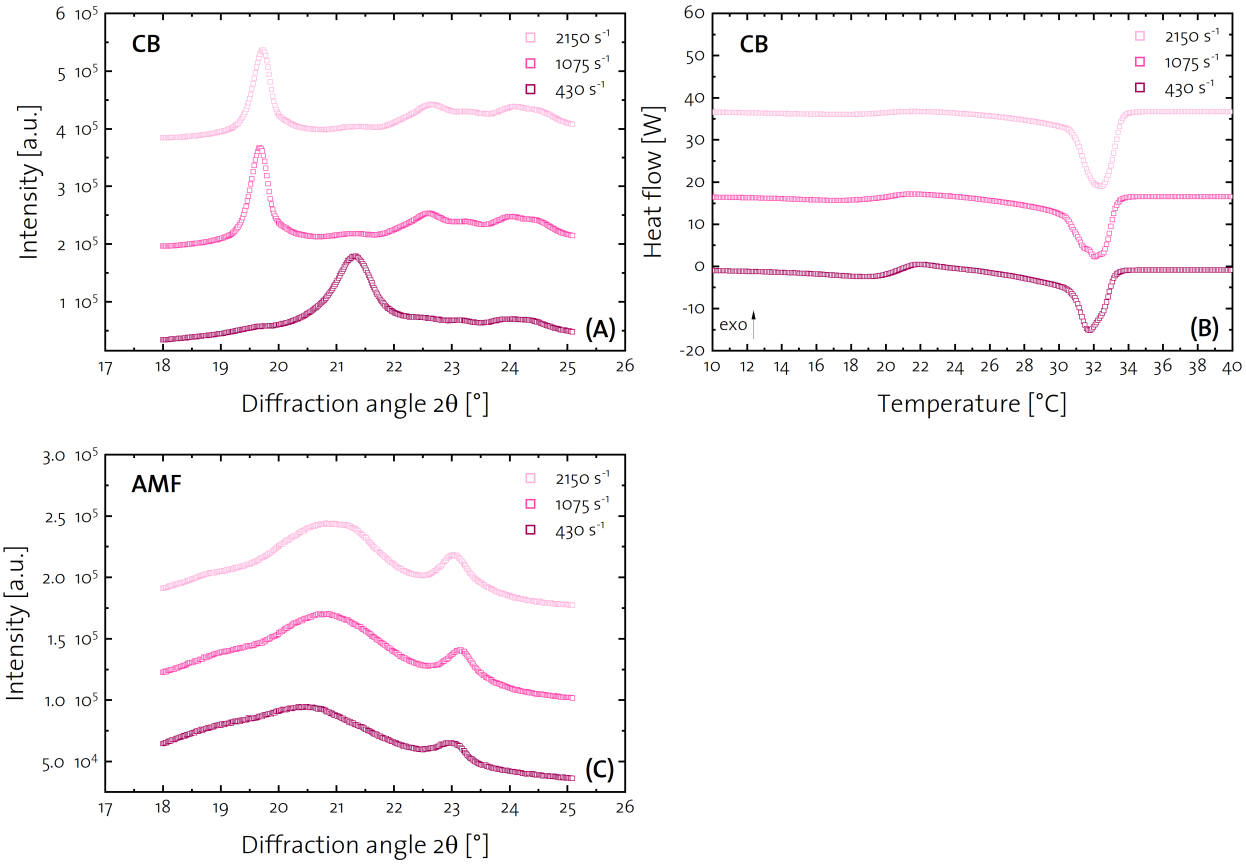

Figure S3: XRD spectra of (A) CB and (C) AMF as well as (B) DSC thermograms of CB directly after crystallization at $\dot{\gamma}_{cryst}$ = 2150, 1075, and 430 s^{-1}.

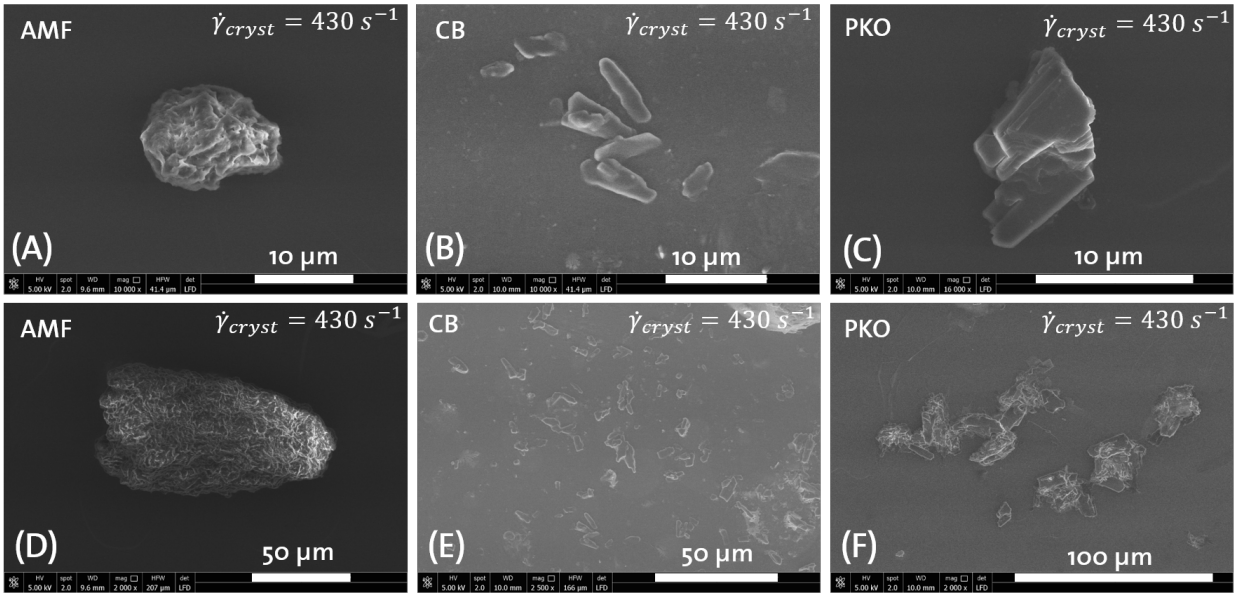

Figure S4: SEM images of (A,D) AMF, (B,E) CB, and (C,F) PKO crystallized at $\dot{\gamma}_{cryst}$ = 430 s^{-1}

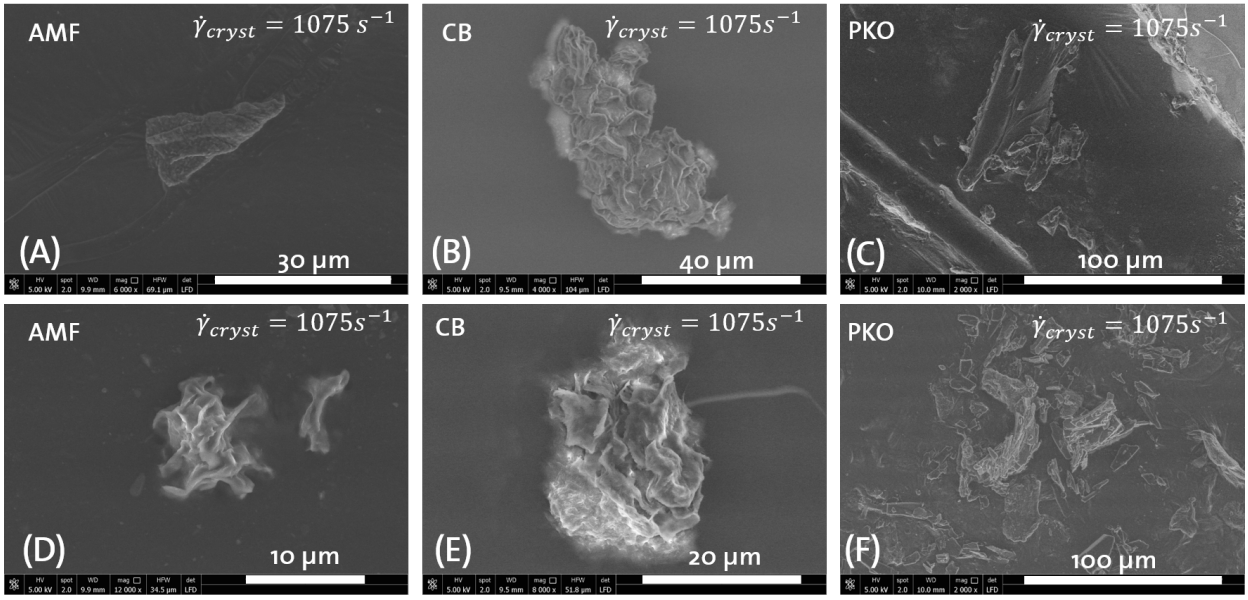

Figure S5: SEM images of (A,D) AMF, (B,E) CB, and (C,F) PKO crystallized at $\dot{\gamma}_{cryst} = 1075\ \mathrm{s}^{-1}$

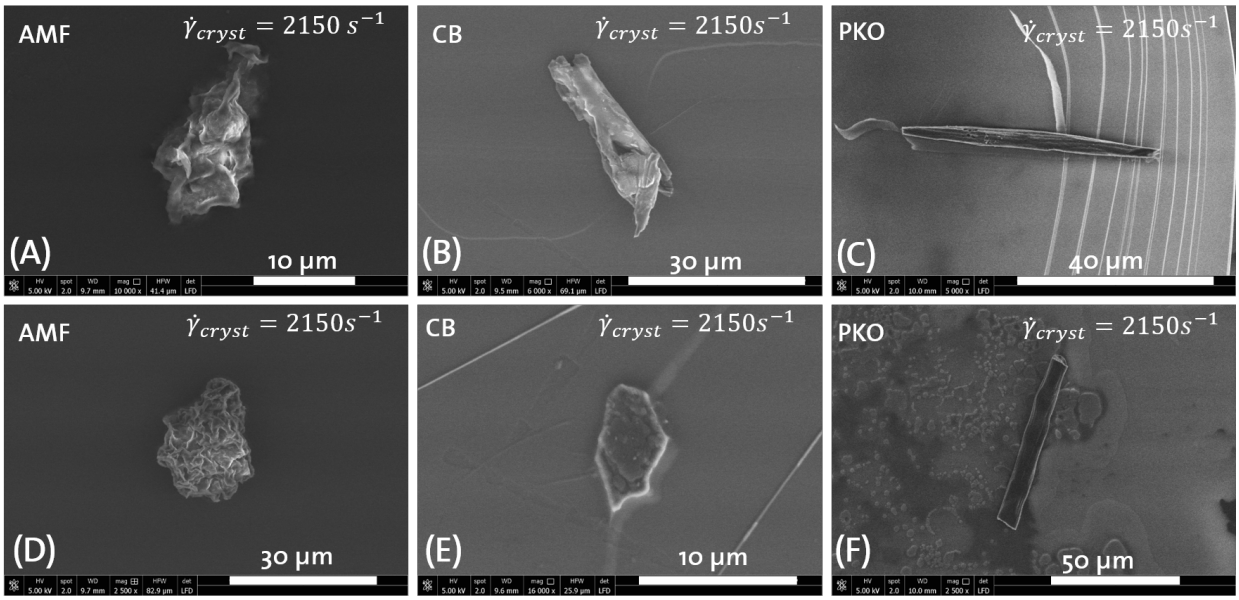

Figure S6: SEM images of (A,D) AMF, (B,E) CB, and (C,F) PKO crystallized at $\dot{\gamma}_{cryst} = 2150\ \mathrm{s}^{-1}$

Table S1: The rotational speed rpm_{inner} of the inner rotating cylinder and the corresponding shear rate in the annular gap $\dot{\gamma}_{gap}$ during foam formation of TAG CMS. The gas volume fraction Φ_g corresponds to the highest achievable gas fraction as function of $\dot{\gamma}_{gap}$ at the indicated crystal volume fraction Φ_{SFC}.

TAG CMS	$\dot{\gamma}_{cryst}$ [s^{-1}]	rpm_{inner} [min^{-1}]	$\dot{\gamma}_{gap}$ [s^{-1}]	Φ_{SFC} [%]	Φ_g [-]
AMF	430	500	275	1.3	0.32
AMF	430	1000	550	4.0	0.39
AMF	430	1000	550	7.2	0.41
AMF	2150	500	275	1.5	0.02
AMF	2150	500	275	4.5	0.11
AMF	2150	500	275	6.2	0.25
CB	430	500	275	1.2	0.42
CB	430	1000	550	5.2	0.43
CB	430	4000	2200	10.3	0.55
CB	2150	200	110	1.7	0.16
CB	2150	1500	825	3.8	0.12
CB	2150	1000	550	9.5	0.06
CB	2150	2000	1100	12.1	0.08
PKO	430	500	275	0.9	0.21
PKO	430	500	275	1.3	0.21
PKO	430	500	275	2.01	0.30
PKO	430	1000	550	2.2	0.36
PKO	430	2000	1100	7.2	0.28
PKO	430	2000	1100	9.2	0.26
PKO	430	3000	1650	12.7	0.28
PKO	2150	500	275	1.7	0.39
PKO	2150	500	275	2.8	0.43
PKO	2150	500	275	3.2	0.58
PKO	2150	1000	550	10.2	0.18
PKO	2150	3000	1650	18.1	0.2

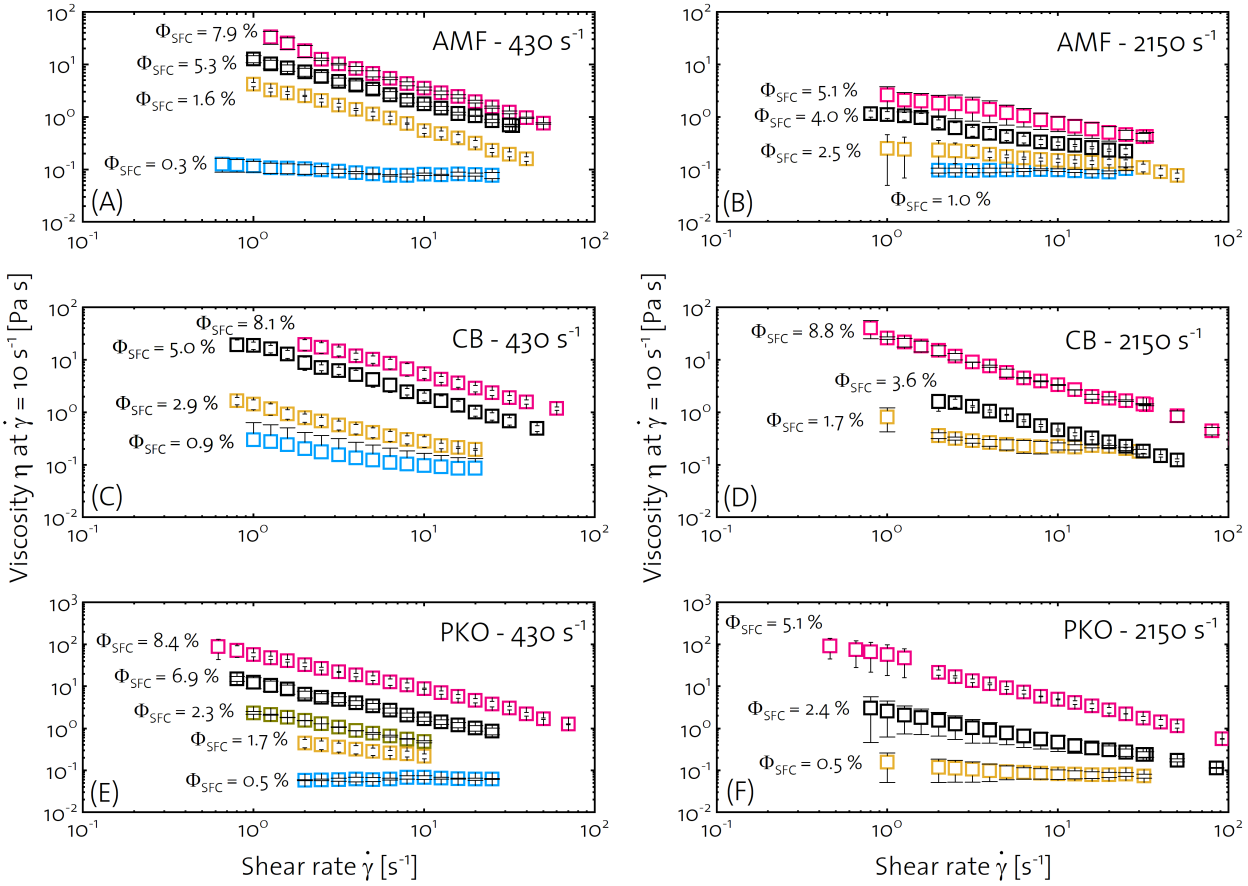

Figure S7: The viscosity η as function of shear rate $\dot{\gamma}$ for TAG CMS composed of (A-B) AMF, (C-D) CB and (E-F) PKO crystallized at 430 and 2150 s^{-1} for varying crystal volume fraction Φ_{SFC}.